J Neuropathol Exp Neurol
Vol. 65, No. 3
March 2006
pp. 245–256

ORIGINAL ARTICLE

Endogenous Cell Repair of Chronic Demyelination

Regina C. Armstrong, PhD, Tuan Q. Le, Nicole C. Flint, Adam C. Vana, and Yong-Xing Zhou, MD, PhD

Abstract

In multiple sclerosis lesions, remyelination typically fails with repeated or chronic demyelinating episodes and results in neurologic disability. Acute demyelination models in rodents typically exhibit robust spontaneous remyelination that prevents appropriate evaluation of strategies for improving conditions of insufficient remyelination. In the current study, we used a mouse model of chronic demyelination induced by continuous ingestion of 0.2% cuprizone for 12 weeks. This chronic process depleted the oligodendrocyte progenitor population and impaired oligodendrocyte regeneration. Remyelination remained limited after removal of cuprizone from the diet. Fibroblast growth factor 2 (FGF2) expression was persistently increased in the corpus callosum of chronically demyelinated mice as compared with nonlesioned mice. We used *FGF2*$^{-/-}$ mice to determine whether removal of endogenous FGF2 promoted remyelination of chronically demyelinated areas. Wild-type and *FGF2*$^{-/-}$ mice exhibited similar demyelination during chronic cuprizone treatment. Importantly, in contrast to wild-type mice, the *FGF2*$^{-/-}$ mice spontaneously remyelinated completely during the recovery period after chronic demyelination. Increased remyelination in *FGF2*$^{-/-}$ mice correlated with enhanced oligodendroglial regeneration. *FGF2* genotype did not alter the density of oligodendrocyte progenitor cells or proliferating cells after chronic demyelination. These findings indicate that attenuating FGF2 created a sufficiently permissive lesion environment for endogenous cells to effectively remyelinate viable axons even after chronic demyelination.

Key Words: Cuprizone, Demyelinating disease, Differentiation, Fibroblast growth factor, Myelin repair, Oligodendrocyte progenitor.

INTRODUCTION

In central nervous system (CNS) demyelinating diseases such as multiple sclerosis (MS), myelin damage impairs impulse conduction along denuded axons. Limited remyelination occurs in MS lesions (1–3) but is typically insufficient to prevent long-term neurologic disability. After a demyelinating event, improved remyelination could maximize functional recovery of viable axons and prevent associated axonal damage and degeneration.

In rodent models, extensive spontaneous remyelination and functional recovery is possible after an episode of acute transient demyelination (4, 5). Proliferation of immature cells and differentiation into myelinating oligodendrocytes is required for this extensive remyelination (6, 7). Similarly, immature oligodendrocyte lineage cells persist in the adult human CNS and may proliferate to increase in number within and near MS lesions (8, 9). However, these immature cells often fail to differentiate sufficiently to remyelinate throughout the extent of MS lesions. Therefore, the repair capacity of endogenous cells may be limited by nonpermissive signals in chronic MS lesions.

Growth factors, cytokines, and cell adhesion molecules may regulate oligodendrocyte progenitor (OP) differentiation into remyelinating oligodendrocytes in the environment of a demyelinated lesion. Among these potential signaling molecules, we have examined the in vivo role of endogenous fibroblast growth factor 2 (FGF2), which is upregulated during postnatal development and in acute demyelination (10–12). During remyelination after acute demyelination, *FGF2* null mice exhibit enhanced oligodendrocyte repopulation of demyelinated lesions (12). This improved oligodendrocyte regeneration was further studied using in vivo retroviral lineage analysis in wild-type versus *FGF2* null mice, which demonstrated that the predominant effect of FGF2 in vivo during remyelination is inhibition of OP differentiation (11).

The current study examines whether this FGF2 effect on OP differentiation and oligodendrocyte regeneration has a significant impact on remyelination. Acute demyelination models in rodents typically exhibit spontaneous remyelination that may be so robust as to prevent appropriate evaluation of strategies for improving remyelination. Therefore, the current study challenges the capacity of endogenous cells to regenerate oligodendrocytes and remyelinate chronically demyelinated lesions.

We induced active demyelination in mice by adding 0.2% cuprizone to the diet so that return to normal chow would allow analysis of spontaneous remyelination without ongoing disease pathogenesis. Cuprizone reproducibly demyelinates the corpus callosum of mice (13). Spontaneous remyelination is greatly reduced after chronic cuprizone demyelination in contrast to acute demyelination (14–16). Importantly, after chronic cuprizone demyelination, axons

From the Department of Anatomy, Physiology, and Genetics (RCA, TQL, NCF, Y-XZ) and the Program in Neuroscience (RCA, NCF, ACV), Uniformed Services University of the Health Sciences, Bethesda, Maryland.
Send correspondence and reprint requests to: Regina C. Armstrong, PhD, Department of Anatomy, Physiology, and Genetics, Uniformed Services University of the Health Sciences, 4301 Jones Bridge Rd., Bethesda, MD 20814-4799; E-mail: rarmstrong@usuhs.mil
This work was supported by National Institutes of Health grant NS39293 and National Multiple Sclerosis Society grant RG3515.

remain viable and can be remyelinated by transplanted OP cells (16). In this chronic demyelination model, the current study demonstrates dramatically improved remyelination by endogenous cells in mice with genetic deletion of *FGF2* as compared with wild-type mice. Thus, FGF2 expression in chronic lesions may limit remyelination and attenuation of FGF2 may generate a sufficiently permissive environment for spontaneous remyelination by endogenous cells.

MATERIALS AND METHODS

Animals

Mice were bred and maintained in the Uniformed Services University of the Health Sciences (USUHS) animal housing facility and all procedures were performed in accordance with guidelines of the National Institutes of Health, the Society for Neuroscience, and the USUHS Institutional Animal Care and Use Committee. *FGF2* knockout mice on the 129 Sv-Ev:Black Swiss genetic background were obtained from breeding heterozygous pairs (provided by Dr. Doetschman, University of Cincinnati). This *FGF2* knockout was generated by a targeted deletion replacing a 0.5-kb portion of the *FGF2* gene, including 121 bp of the promoter and the entire first exon with an *Hprt* minigene (17).

Cuprizone Experimental Demyelination

Cuprizone ingestion results in a reproducible pattern of extensive corpus callosum demyelination (12, 13). Cuprizone treatment was started at 8 weeks of age and only male mice were used. Cuprizone (0.2% (w/w), finely powdered oxalic bis(cyclohexylidenehydrazide) (Sigma-Aldrich, St. Louis, MO), was thoroughly mixed into chow (diet TD.01453; Harlan Teklad, Madison, WI), which was available ad libitum. Mice were maintained on the cuprizone diet until perfused for analysis or returned to normal chow after 6 weeks or 12 weeks of cuprizone ingestion.

Tissue Preparation

Mice were perfused with 4% paraformaldehyde and then brains were dissected before overnight postfixation in 4% paraformaldehyde (18). Brain tissue was cryoprotected overnight at 4°C in 30% sucrose and frozen in OCT compound for immunostaining and in situ hybridization.

In Situ Hybridization

In situ hybridization and preparation of digoxigenin-labeled riboprobes were performed as previously detailed (18, 19). Antisense riboprobes were used to detect mRNA transcripts for proteolipid protein (PLP; gift from Dr. Lynn Hudson; National Institutes of Health [20]) and PDGFαR (gift from Dr. Bill Richardson; University College London [21]). The digoxigenin-labeled riboprobes were hybridized to 15-μm-thick coronal brain sections. Digoxigenin was detected with an alkaline phosphatase-conjugated sheep antidigoxigenin antibody (Boehringer Mannheim, Indianapolis, IN) followed by reaction with NBT/BCIP substrate (DAKO, Carpinteria, CA).

Immunohistochemistry

To identify OPs in situ, 15-μm coronal brain sections were immunostained for NG2 and PDGFαR (12, 19). Primary antibodies used were rabbit polyclonal antiNG2 antibody (gift from Dr. William Stallcup, La Jolla, CA) and rat monoclonal antiPDGFαR antibody (APA5; Pharmingen, San Diego, CA). Donkey antirabbit IgG $F(ab')_2$ conjugated with Cy3 (Jackson Immunoresearch, West Grove, PA) was used to detect NG2, whereas the PDGFαR was detected with biotinylated donkey antirat IgG $F(ab')_2$ (Jackson Immunoresearch) followed by coumarin tyramide amplification (New England Nuclear, Boston, MA).

Myelin was immunostained with monoclonal antibody 8-18C5, which recognizes myelin oligodendrocyte glycoprotein (MOG). Hybridoma cells were provided by Dr. Minetta Gardinier, University of Iowa (22). MOG immunolabeling was detected with donkey antimouse IgG $F(ab')_2$ conjugated with Cy3 (Jackson Immunoresearch).

Cell proliferation was estimated with immunostaining for Ki-67 antigen, which is expressed in the nuclei of actively dividing cells but absent at G_0 (23). Ki-67 was recognized with a rat monoclonal antibody to mouse Ki-67 antigen (DAKO) followed by detection with the ABC elite kit using 3,3-diaminobenzidine (DAB) as a substrate (Vector Labs, Burlingame, CA).

Imaging, Quantification, and Statistical Analysis

Images of in situ hybridization and immunostaining results were captured with a Spot 2 CCD digital camera using Spot Advanced image acquisition software (Diagnostic Instruments, Sterling Heights, MI) on an Olympus IX-70 microscope. Images were prepared as panels using Adobe Photoshop (San Jose, CA).

For comparing cell densities, all quantification was performed by an investigator blinded to the treatment condition. Cells expressing PLP mRNA were quantified using unbiased stereologic morphometric analysis (12) (Stereologer System from Systems Planning and Analysis, Inc., Alexandria, VA). Analysis was restricted to the corpus callosum region from the midline and extending laterally to below the cingulum in 15-μm-thick coronal sections. Using the Stereologer System, the specimen thickness contributes to the sampled volume so that measurements reflect cells/mm^3. The unbiased stereologic method could not be used appropriately for conditions with relatively few cells of interest in any chosen category. Therefore, quantification of cells in the corpus callosum expressing PDGFαR or Ki-67 required counting all labeled cells and using the Spot 2 CCD camera and software to measure the area sampled, resulting in density units of cells/mm^2 (12).

Quantification of corpus callosum myelination was estimated from MOG immunofluorescence detected with a Spot 2 CCD camera. Using Metamorph software, pixel intensity values were normalized between sections by thresholding to exclude values below the level of immunoreactivity in the dorsal fornix, which was selected as an adjacent white matter tract that is not demyelinated by cuprizone. The percent area of the corpus callosum (midline

bilaterally to a point under the cingulum apex) with MOG immunoreactivity above the threshold level was then used as an estimate of the myelinated area.

Each category analyzed included three or more tissue sections per mouse and three or more mice per condition, except where larger sample sizes are noted in text and/or figure legends. One-way analysis of variance (ANOVA) with post hoc Tukey's multiple comparison test was used to determine significant differences among stages of disease progression or treatment. Unpaired Student *t*-test was used to compare between *FGF2* genotypes in nonlesioned mice. Significance of an *FGF2* genotype effect across multiple treatment conditions was calculated using a two-way ANOVA. No statistical comparisons were made between mice with different genetic backgrounds (i.e. C57Bl/6 mice and *FGF2* mice).

RESULTS

Chronic Cuprizone Demyelination Provided a Relevant Model of Insufficient Remyelination to Characterize the Repair Capacity of Endogenous Cells

C57Bl/6 mice were used to establish parameters for analyzing, and later manipulating, the capacity of endogenous

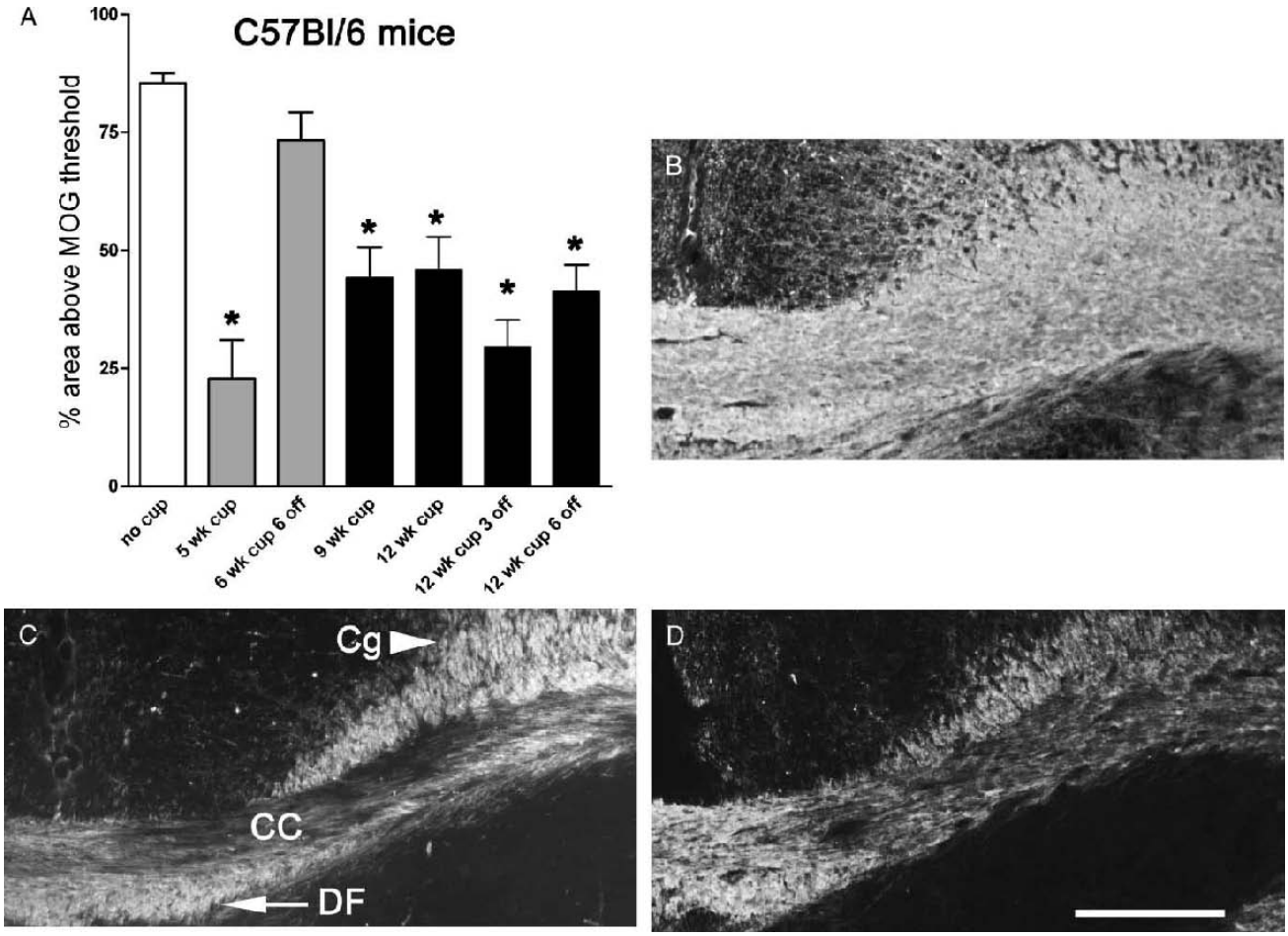

FIGURE 1. Spontaneous remyelination of the corpus callosum was compromised after chronic demyelination of C57Bl/6 mice. **(A)** Corpus callosum myelination was estimated by immunofluorescence for myelin oligodendrocyte glycoprotein (MOG). Pixel intensity values were normalized between tissue sections by thresholding to exclude values below the immunoreactivity in the dorsal fornix, which was not demyelinated by cuprizone (see DF in **[C]**). The percent area of the corpus callosum with MOG immunoreactivity above the threshold level was then used as an estimate of myelinated area. Bar colors indicate treatment conditions: no cuprizone (white), acute cuprizone (up to 6 weeks, gray), or chronic cuprizone (9 weeks and above, black). At least three sections were quantified per mouse and at least four mice per condition. After acute cuprizone, myelination returned to near nonlesioned values ($p > 0.05$; no cuprizone, n = 4; 6 weeks cuprizone 6 weeks off, n = 5). Recovery to nonlesioned levels did not occur after chronic cuprizone ($p < 0.001$; 12 weeks cuprizone 6 weeks off; n = 6). Values for 12-week cuprizone three off were not significantly different than either 12-week cuprizone or 12-week cuprizone 6 off. Significant differences, $p < 0.05$ or less, are noted by an asterisk (*) for comparisons with no cuprizone. **(B–D)** Representative MOG immunostaining of coronal sections through the corpus callosum. **(B)** Control without cuprizone treatment (age matched to **[D]**). **(C)** Continuous cuprizone for 12 weeks. **(D)** continuous cuprizone for 12 weeks followed by 6 weeks of recovery on normal chow. Midline at left side of each image. CC, corpus callosum; DF, dorsal fornix; Cg, cingulum. Scale bar for **(B, C, D)** shown in **(D)** = 250 μm.

oligodendrocyte lineage cells to repopulate and remyelinate chronically demyelinated lesions. We used the cuprizone model to take advantage of the ability to stop active demyelination simply by returning the mice to a normal diet. As characterized in C57Bl/6 mice, continuous cuprizone ingestion results in persistent demyelination with a variable degree of partial remyelination, indicating a regenerative potential of endogenous cells even while mice are still fed cuprizone (24). However, after 12 weeks of continuous 0.2% cuprizone ingestion in C57Bl/6 mice, spontaneous remyelination remained limited through the 6-week recovery period (Fig. 1). This poor remyelination after chronic demyelination contrasted with the almost complete remyelination seen within the same recovery period after acute demyelination (i.e. 6 weeks on cuprizone followed by 6 weeks off cuprizone; Fig. 1).

Persistent but Limited Endogenous Oligodendrocyte Lineage Cell Regenerative Capacity After Chronic Demyelination

To better evaluate the underlying causes of limited remyelination after chronic demyelination, we characterized the oligodendrocyte lineage cell responses relative to disease progression with a focus on the repair potential. Oligodendrocyte and OP populations were characterized during multiple stages of disease progression: nonlesioned (no cuprizone), acute demyelination (3–5 weeks of continuous cuprizone), chronic demyelination (12 weeks of continuous cuprizone), and recovery after chronic demyelination (12 weeks of continuous cuprizone followed by normal chow for 3 or 6 weeks). In situ hybridization was used to identify oligodendrocytes expressing PLP mRNA transcripts (Fig. 2) and OP cells expressing

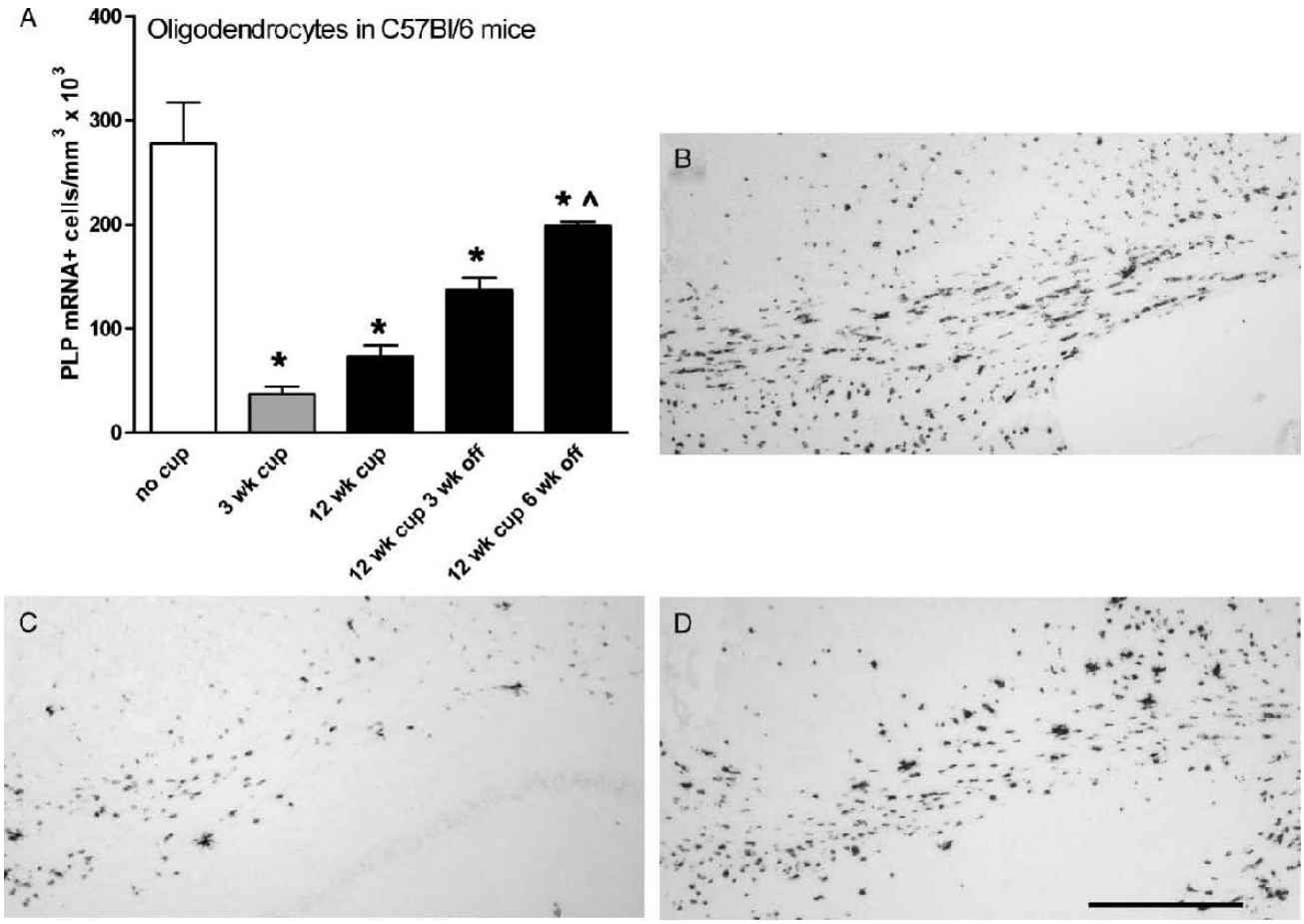

FIGURE 2. Oligodendroglial repopulation of the corpus callosum was compromised after chronic demyelination of C57Bl/6 mice. **(A)** Quantification of the density of oligodendrocytes in the corpus callosum of C57Bl/6 mice. In situ hybridization for PLP mRNA, which identifies premyelinating and myelinating oligodendrocytes, was quantified using unbiased stereology with at least three sections per mouse and at least four mice per condition. Bar colors indicate no cuprizone (white), acute cuprizone (gray), or chronic cuprizone (black). The oligodendrocyte density after 12 weeks of cuprizone followed by 6 weeks for recovery was still significantly below nonlesioned values ($p > 0.05$; $n = 5$ for both conditions). Significant differences, $p < 0.05$ or less, are noted by an asterisk (*) for comparisons with no cuprizone and with a carrot (^) for comparisons of recovery stages with 12 week cuprizone. **(B–D)** Representative PLP in situ hybridization of coronal sections through the corpus callosum. **(B)** Control without cuprizone treatment (age matched to **[D]**). **(C)** Continuous cuprizone for 12 weeks. **(D)** Continuous cuprizone for 12 weeks followed by 6 weeks of recovery on normal chow. Midline is at left side of each image and areas are similar to those shown Figure 1. Scale bar for **(B, C, D)** shown in **(D)** = 250 μm.

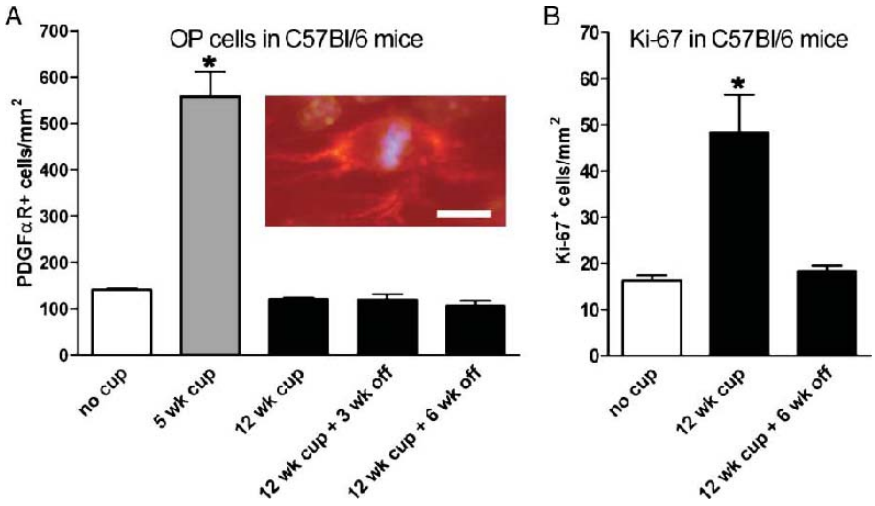

FIGURE 3. Chronic demyelination compromised oligodendrocyte progenitor (OP) and cycling cell densities. **(A, B)** Quantification of the density of OP cells (**[A]**, identified by in situ hybridization for PDGFαR mRNA) and cycling cells (**[B]**, detected by Ki-67 immunostaining) in the corpus callosum of C57Bl/6 mice. Bar colors indicated no cuprizone (white), acute cuprizone (gray), or chronic cuprizone (black). At least three sections were quantified per mouse and at least four mice per condition. **(A)** The density of PDGFαR+ cells was significantly increased during acute demyelination but decreased to nontreated levels during chronic cuprizone administration ($p < 0.001$ for 5 weeks cuprizone, denoted by asterisk [*], in comparison with all other conditions; $p > 0.05$ for each comparison of chronic cuprizone with no treatment; no cuprizone, n = 5; 5 weeks cuprizone, n = 5; 12 weeks cuprizone, n = 4; 12 weeks cuprizone + 3 weeks off, n = 6; 12 weeks cuprizone + 6 weeks off, n = 3). **(B)** The density of Ki-67+ cells indicated a significant increase in the population of cycling cells after 12 weeks of cuprizone that declined during the recovery phase ($p < 0.01$ for 12 weeks cuprizone, denoted by asterisk (*), in comparison with all other conditions; no cuprizone, n = 4; 12 weeks cuprizone, n = 5; 12 weeks cuprizone + 6 weeks off, n = 5). (**A**, inset) Example of a cell immunolabeled for NG2 (red) and exhibiting a chromatin arrangement (blue, DAPI staining) that was characteristic of metaphase and indicative of active mitosis. Scale bar for inset in **(A)** = 10 μm.

platelet-derived growth factor α receptor (PDGFαR) mRNA transcripts (Fig. 3).

Quantitative analysis of the oligodendrocyte population revealed ongoing partial regeneration during and after chronic demyelination (Fig. 2). The oligodendrocyte density was lowest after the initial 3 weeks of cuprizone in the acute phase. After 12 weeks of continuous cuprizone, the oligodendrocyte density continued to be severely reduced relative to values from nontreated mice. Ongoing partial regeneration during chronic demyelination was indicated by the fact that the oligodendrocyte density after 12 weeks was higher than after the initial 3 weeks. After ending the chronic cuprizone treatment, this oligodendrocyte regeneration improved during the recovery period. Interestingly, as shown in Figure 1, remyelination did not progress similarly during this 6-week recovery period. The PLP mRNA in situ hybridization used to identify oligodendrocytes should detect both premyelinating and myelinating oligodendrocytes because PLP transcription

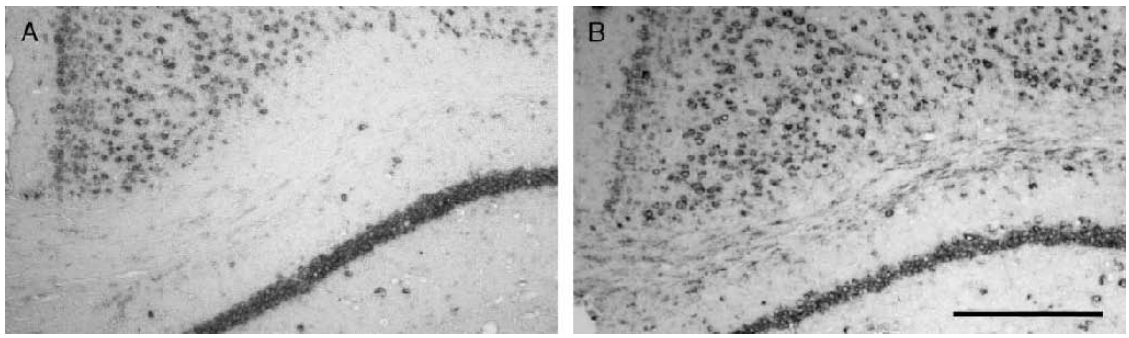

FIGURE 4. In chronically demyelinated corpus callosum of C57Bl/6 mice, FGF2 expression continued to be upregulated in lesions. **(A, B)** Representative coronal sections through the corpus callosum with the midline along the left edge of each image. In situ hybridization for FGF2 mRNA showed many labeled cells in neuronal structures, for example, cortex (above corpus callosum) and hippocampus (below corpus callosum). In the corpus callosum, few cells exhibited detectable FGF2 mRNA in nontreated mice **(A)** but FGF2 mRNA expression was markedly increased in the corpus callosum of mice fed 0.2% cuprizone for 12 weeks **(B)**. Scale bar for **(A, B)** shown in **(B)** = 250 μm.

precedes myelin formation (25). These results indicate that after chronic demyelination, a proportion of premyelinating oligodendrocytes that are generated during the recovery period may fail to differentiate into myelinating oligodendrocytes.

The OP population dynamics were dramatically different in response to acute versus chronic demyelination (Fig. 3). In response to the initial episode of acute demyelination, the OP population was amplified almost fourfold (Fig. 3). However, by the end of the chronic demyelination period, the OP density was greatly reduced and remained low during the recovery period. In the chronic lesions, similar results were observed with OP identification using PDGFαR (Fig. 3A) and using NG2 (12 weeks cuprizone = 155 cells/mm^2, n = 5; 12 weeks cuprizone plus 3 weeks recovery

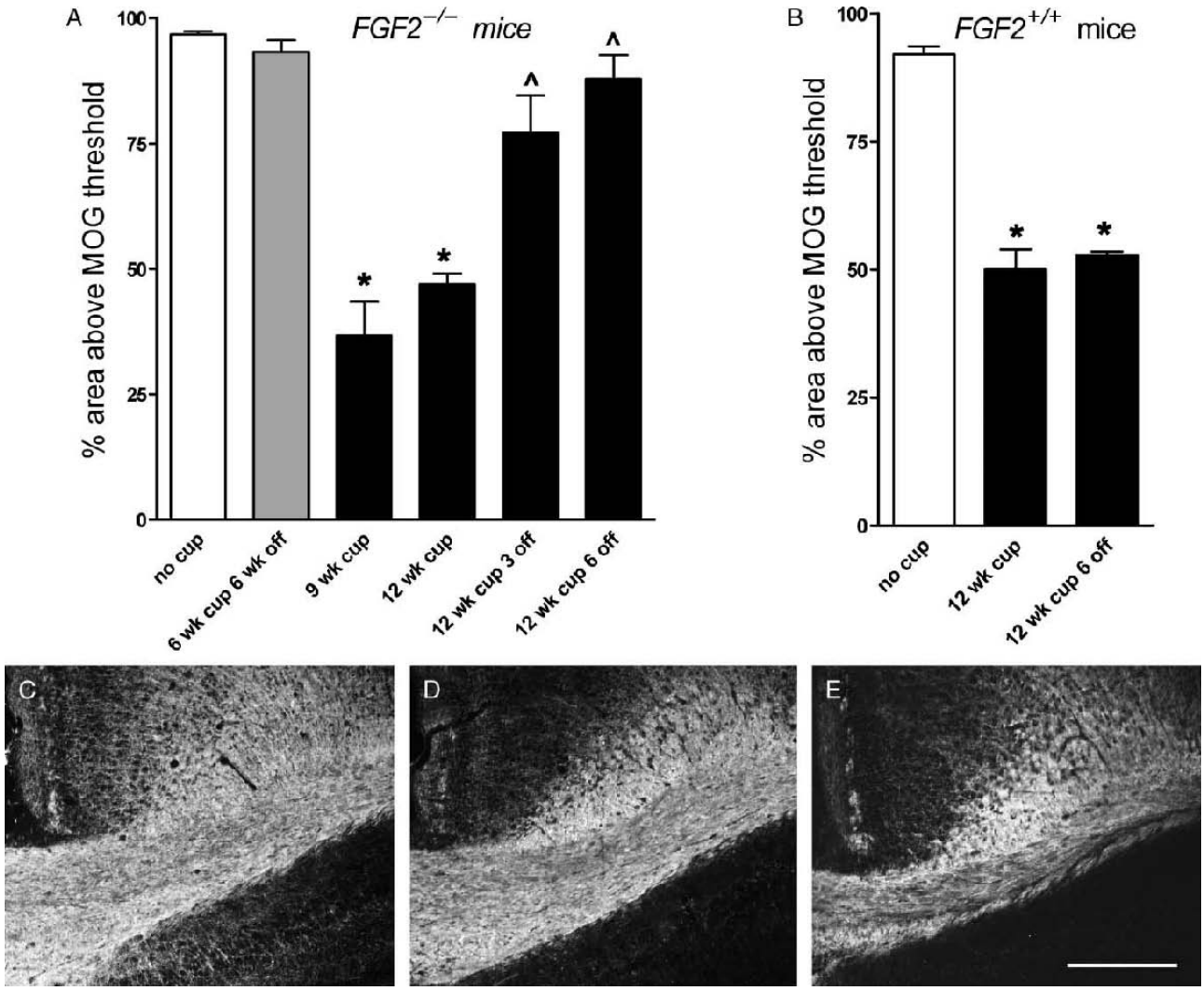

FIGURE 5. Spontaneous remyelination of the corpus callosum after chronic demyelination in *FGF2* null mice but not in *FGF2* wild-type mice. **(A, B)** Quantification (like in Figure 1) of corpus callosum myelination estimated by immunostaining for myelin oligodendrocyte glycoprotein (MOG) in cuprizone-treated *FGF2*$^{-/-}$ mice **(A)** and *FGF2*$^{+/+}$ mice **(B)**. The corpus callosum showed persistent demyelination with 0.2% cuprizone ingestion throughout 9 weeks and 12 weeks. After 12 weeks of cuprizone treatment, on return to normal chow, remyelination in *FGF2*$^{-/-}$ mice significantly improved ($p < 0.001$; 12 weeks cuprizone, n = 4; 12 weeks cuprizone 6 weeks off, n = 4) and recovered to nonlesioned levels ($p > 0.05$; no cuprizone, n = 5; 12 weeks cuprizone 6 weeks off). In contrast, values in *FGF2*$^{+/+}$ mice did not increase after chronic demyelination ($p > 0.05$; 12 weeks cuprizone, n = 4 vs. 12 weeks cuprizone 6 weeks off, n = 3) and remained significantly below nonlesioned levels ($p < 0.001$; no cuprizone, n = 5 vs. 12 weeks cup). Significant differences, $p < 0.05$ or less, are noted by an asterisk (*) for comparison with no cuprizone and with a carrot (^) for comparisons of recovery stages with 12 weeks cuprizone. Comparison of the *FGF2*$^{+/+}$ values with the matching set of conditions in *FGF2*$^{-/-}$ mice demonstrated a significant effect of genotype ($p < 0.0001$). **(C–E)** Representative coronal sections of MOG immunostaining. Midline is at left side of each image and areas are similar to those shown Figure 1. **(C)** *FGF2*$^{-/-}$control mouse without cuprizone treatment (age matched to **[D]**). **(D)** *FGF2*$^{-/-}$ mouse after 12 weeks of cuprizone followed by 6 weeks on normal chow. **(E)** *FGF2*$^{+/+}$ mouse after 12 weeks of cuprizone followed by 6 weeks on normal chow. Scale bar for **(C–E)** shown in **(E)** = 250 μm.

= 169 cells/mm^2, n = 6; 12 weeks cuprizone plus 6 weeks recovery = 115 cells/mm^2, n = 5). At 12 weeks of cuprizone treatment, very few cells in the corpus callosum were identified as actively undergoing mitosis using DAPI counterstaining to reveal mitotic chromatin figures, but each actively dividing cell was also immunostained for NG2 (inset, Fig. 3A). Immunostaining for Ki-67 nuclear antigen was used to more broadly identify actively cycling cells within the corpus callosum (Fig. 3B). Ki-67-labeled cycling cells were present at less than half the density of OP cells. This cycling population, although still relatively small, was significantly increased within the corpus callosum of mice fed cuprizone for 12 weeks as compared with age-matched controls or with mice that had recovered for 6 weeks after chronic demyelination. Together, these findings demonstrated compromised but continued OP cycling and regeneration of oligodendrocytes during chronic demyelination and the subsequent recovery period (Figs. 2, 3).

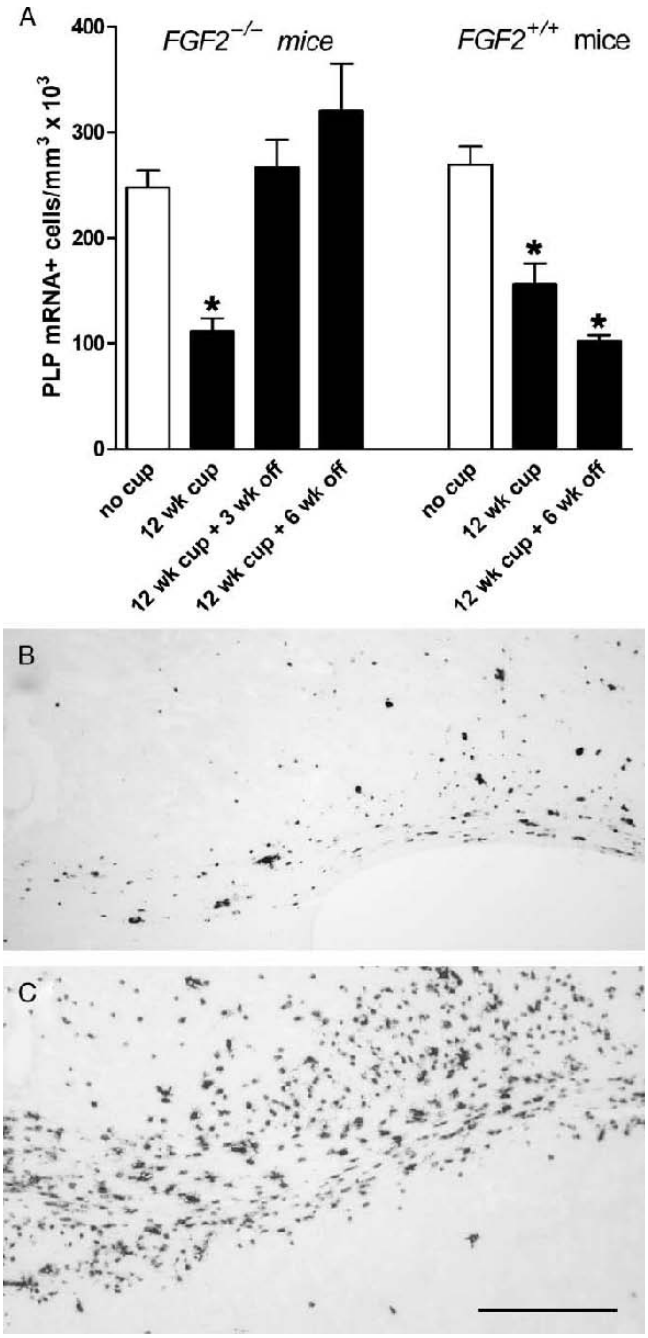

FGF2 Expression Was Elevated in Chronically Demyelinated Lesions

FGF2 expression is increased during acute cuprizone demyelination and can inhibit OP differentiation and oligodendrocyte regeneration during subsequent remyelination (11, 12). Using in situ hybridization for FGF2 mRNA transcripts, we have shown that elevated FGF2 expression persists within chronic cuprizone lesions, as compared with nonlesioned corpus callosum (Fig. 4). FGF2 mRNA transcript abundance related to changes in FGF2 protein detection in developing white matter and after acute demyelination (10, 19). We predicted that in chronic lesions, FGF2 inhibition of differentiation could contribute to the limited capacity to generate remyelinating oligodendrocytes (Figs. 1, 2), especially in the context of a reduce OP pool (Fig. 3A).

Removal of Endogenous FGF2 Promoted Spontaneous Remyelination After Chronic Demyelination

Although the endogenous populations did not efficiently remyelinate after chronic cuprizone demyelination in C57Bl/6 mice (Fig. 1), transplantation of OP cells has shown that the axons remain viable for remyelination (16). Therefore, we used this chronic demyelination model in *FGF2*

FIGURE 6. Oligodendroglial repopulation of the corpus callosum after chronic demyelination was dramatically improved in *FGF2*$^{-/-}$ mice as compared with *FGF2*$^{+/+}$ mice. **(A)** Quantification of the density of oligodendrocytes in the corpus callosum of *FGF2* mice. In situ hybridization for PLP mRNA, which identified premyelinating and myelinating oligodendrocytes, was quantified using unbiased stereology with at least three sections per mouse and at least four mice per condition. The oligodendrocyte density after 12 weeks of continuous cuprizone was significantly below nonlesioned values (noted by asterisks [*]; $p < 0.01$ for *FGF2*$^{+/+}$; $p < 0.05$ for *FGF2*$^{-/-}$ mice; n = 4 for each condition). After 12 weeks of cuprizone and a subsequent 3- and 6-week period for recovery on normal chow, oligodendrocyte densities in *FGF2*$^{-/-}$ mice were no longer significantly different as compared with nonlesion values ($p > 0.05$ at 3 weeks and at 6 weeks; n = 4 for each condition). Comparison of the *FGF2*$^{+/+}$ values with the matching conditions in *FGF2*$^{-/-}$ mice demonstrated a significant effect of genotype ($p = 0.0196$). **(B, C)** Representative PLP in situ hybridization of coronal sections through the corpus callosum of an *FGF2*$^{+/+}$ mouse **(B)** and an *FGF2*$^{-/-}$ mouse **(C)**. Midline is at the left side of each image and areas are similar to those shown Figure 1. In both micrographs **(B, C)**, sections shown are from mice that were fed cuprizone continuously for 12 weeks followed by 6 weeks on normal chow. Scale bar for **(B, C)** shown in **(C)** = 250 μm.

knockout mice to test whether repair from the endogenous OP population might be improved by removing endogenous FGF2 from the lesion environment. The extent of demyelination after 12 weeks of cuprizone ingestion was similar in C57Bl/6 mice and mice of both *FGF2* wild-type ($FGF2^{+/+}$) and null ($FGF2^{-/-}$) genotypes (Figs. 1, 5). The percentage of the corpus callosum area with myelin immunolabeling was 45.8 ± 14.1% in C57Bl/6 mice, 50.05 ± 7.8% in $FGF2^{+/+}$ mice, and 46.9 ± 4.3% in $FGF2^{-/-}$mice. After the chronic demyelination, only in $FGF2^{-/-}$ mice did myelin immunostaining in the corpus callosum significantly increase during the recovery period (Fig. 5). Surprisingly, the myelin immunostaining recovered to approximately nonlesion levels by 6 weeks after removal of cuprizone from the diet of $FGF2^{-/-}$ mice. In contrast, in C57Bl/6 mice (Fig. 1) or $FGF2^{+/+}$ mice (Fig. 5), the myelinated proportion of corpus callosum area did not significantly increase during the recovery period.

After Chronic Demyelination, the Density of Oligodendrocytes Recovered in the Absence of FGF2

This striking improvement in remyelination corresponded with a dramatic increase in oligodendrocyte repopulation of chronic lesions in $FGF2^{-/-}$ mice, which was not found in $FGF2^{+/+}$ mice (Fig. 6). Before cuprizone treatment, nonlesioned $FGF2^{+/+}$ and $FGF2^{-/-}$ mice had a similar density of oligodendrocytes in the corpus callosum at 26 weeks of age, which corresponded with the longest cuprizone treatment and recovery protocol. In addition, the cuprizone-induced loss of oligodendrocytes in $FGF2^{+/+}$ and $FGF2^{-/-}$ mice was similar at the end of the chronic cuprizone treatment. In conjunction with the quantitative myelin immunostaining analysis, these findings indicate that

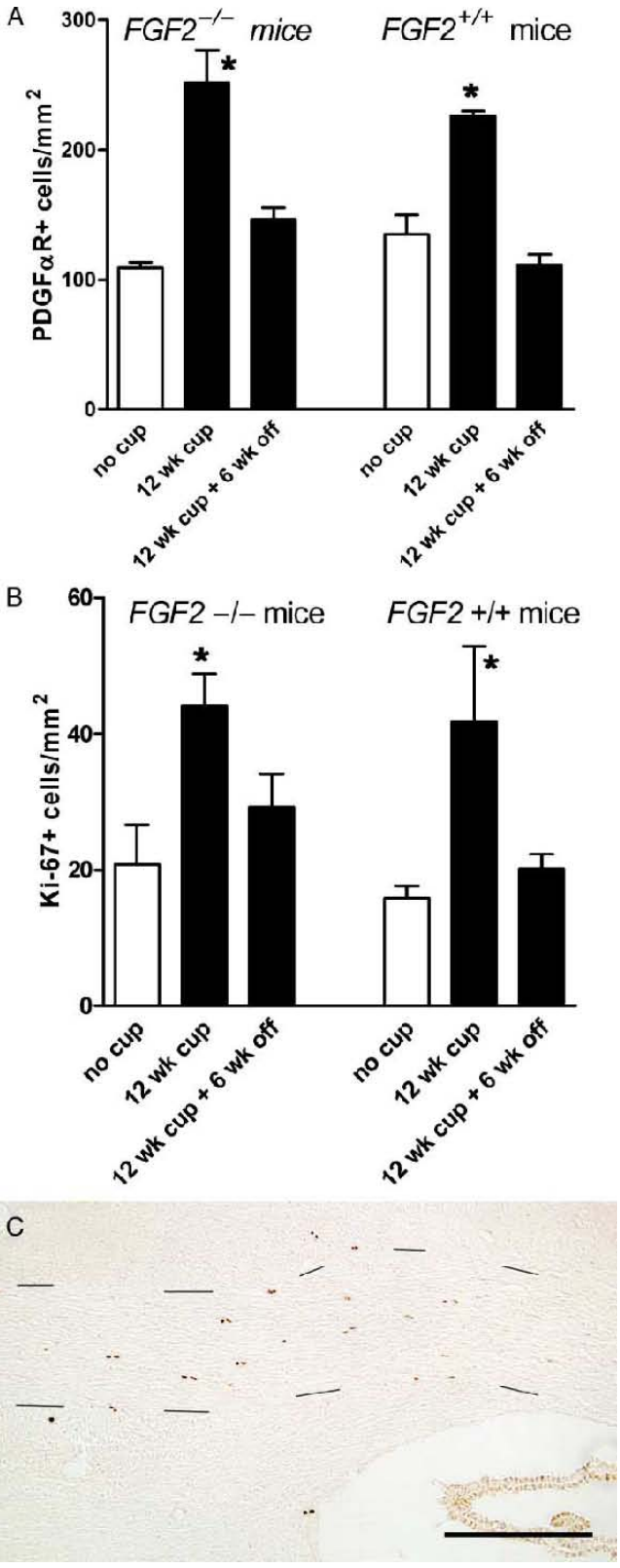

FIGURE 7. Oligodendrocyte progenitor (OP) and cycling cell populations in corpus callosum after chronic demyelination were not altered by *FGF2* genotype. **(A, B)** Quantification of the density of OP cells (**[A]**, identified by in situ hybridization for PDGFαR) and cycling cells (**[B]**, identified by Ki-67 immunostaining) in corpus callosum white matter of $FGF2^{+/+}$ mice and $FGF2^{-/-}$ mice. **(A)** Compared with nontreated mice, the density of OP cells was significantly higher after chronic (12 weeks) cuprizone regardless of *FGF2* genotype (noted by asterisks [*]; $FGF2^{+/+}$ mice, $p < 0.001$; $FGF2^{-/-}$ mice, $p < 0.001$; $n = 4$ for each condition). **(B)** The density of cycling cells was also similarly increased significantly after 12 weeks of cuprizone, relative to nontreated mice, for both *FGF2* genotypes (noted by asterisks [*]; $FGF2^{+/+}$ mice, $p < 0.05$; $FGF2^{-/-}$ mice, $p < 0.05$; $n = 5$ for each no cuprizone genotype, $n = 4$ for each 12 week cuprizone genotype). Comparison of all three $FGF2^{-/-}$ conditions with those from $FGF2^{+/+}$ mice demonstrated no significant effect of genotype for PDGFαR+ cells ($p = 0.2746$) or Ki-67+ cells ($p = 0.8651$). **(C)** Representative example of Ki-67 immunostaining of coronal sections through the corpus callosum of an $FGF2^{-/-}$ mouse after 12 weeks of chronic cuprizone. Midline is at the left side of each image and areas are similar to those shown Figure 1. The corpus callosum was approximately within the borders demarcated between the dashed lines. Scale bar in **(C)** = 250 μm.

FGF2$^{+/+}$ and *FGF2*$^{-/-}$ mice experienced a similar chronic disease severity. Importantly, during the 6-week recovery period after chronic demyelination, the oligodendrocyte density returned to nonlesioned values in the *FGF2*$^{-/-}$ mice, but not in *FGF2*$^{+/+}$ mice. Analysis of an additional intermediate recovery period in *FGF2*$^{-/-}$ mice confirmed this increased oligodendrocyte regeneration and demonstrated that this repopulation could occur within 3 weeks after removal of cuprizone from the diet.

FGF2 Genotype Did not Regulate the Density of Progenitor and Cycling Cell Populations

We previously showed that the absence of FGF2 did not significantly alter OP amplification in response to acute cuprizone demyelination (12). A robust OP proliferative response occurred after 5 weeks of cuprizone in *FGF2* null and wild-type mice that was similar to the previously mentioned data for C57Bl/6 mice (Fig. 3). However, the OP population was depleted during chronic demyelination in contrast to the amplified OP response to acute demyelination in C57Bl/6 (Fig. 3). Therefore, we examined the effect of *FGF2* genotype on the density of OP cells and cycling cells in the corpus callosum after chronic demyelination. *FGF2* genotype did not appear to alter the OP population dynamics of chronically demyelinated mice or age-matched nonlesioned mice (Fig. 7). The density of OP cells, identified by in situ hybridization for PDGFαR mRNA, was similar in *FGF2*$^{+/+}$ mice and *FGF2*$^{-/-}$ mice (Fig. 7A). Somewhat unexpectedly, mice of both *FGF2* null and wild-type genotypes, which are on a 129 Sv-Ev:Black Swiss genetic background, exhibited an increase in OP cell density after 12 weeks of cuprizone that was not observed in C57Bl/6 mice (Fig. 3A). This strain difference in OP accumulation after chronic demyelination corresponded with fewer oligodendrocytes observed during the recovery period in *FGF2*$^{+/+}$ mice (Fig. 6) as compared with C57Bl/6 mice (Fig. 2). Therefore, the *FGF2* background appears to be even less favorable than the C57Bl/6 background for OP differentiation and oligodendrocyte regeneration, yet the detrimental effects of the chronic lesion environment can still be overcome in the *FGF2*$^{-/-}$ mice.

Ki-67 immunostaining (Fig. 7C) indicated that the density of cycling cells in the corpus callosum was less than 20% of the density of OP cells, indicating a relatively low level of ongoing proliferation. Cells with nuclear Ki-67 immunoreactivity were often observed as doublets, as is appropriate for confirming detection of a cycling population. The density of cells immunolabeled for Ki-67 nuclear antigen increased in chronically lesioned corpus callosum with a return to nonlesioned levels during the recovery phase. The density of endogenous cells that were proliferating in the corpus callosum of *FGF2*$^{-/-}$ mice was similar to the values for *FGF2*$^{+/+}$ mice (Fig. 7B) and for C57Bl/6 mice (Fig. 3). The similarity of *FGF2*$^{-/-}$ mice and *FGF2*$^{+/+}$ mice in our analysis of OP cells and cycling cells indicates that the dramatic differences observed in oligodendrocytes and remyelination may result from a permissive effect of FGF2 removal on OP differentiation into remyelinating oligodendrocytes.

DISCUSSION

In MS lesions, an initial episode of transient demyelination may be followed by spontaneous remyelination. However, remyelination typically fails with recurring or chronic myelin damage. The current studies show the advantages of the cuprizone model of chronic demyelination for focusing on this compromised repair response. Importantly, our analysis in *FGF2*$^{-/-}$ mice demonstrates that it is possible to overcome chronic lesion effects on endogenous oligodendrocyte lineage cells to increase remyelination. More specifically, taken together with our previous work (11, 12), our findings in *FGF2*$^{-/-}$ mice indicate that removing FGF2 inhibition of OP differentiation promotes spontaneous remyelination from a depleted pool of endogenous progenitors that persists after chronic demyelination.

The current findings in C57Bl/6 mice are consistent with previous reports of cuprizone treatment causing extensive demyelination of the corpus callosum in this mouse strain (13, 16, 24, 26). To take further advantage of this model for examining mechanisms to promote remyelination from endogenous cells, we have further characterized the endogenous oligodendrocyte lineage population responses during the recovery period. We used C57Bl/6 mice for this part of our study to facilitate comparison with other studies, because differences in mouse strain can influence the response to cuprizone as well as overall cellular responses to CNS injury (13, 27). After a transient episode of demyelination from 6 weeks of cuprizone ingestion, spontaneous remyelination is effective throughout the corpus callosum. In contrast, after a prolonged period of demyelination, from 12 weeks of continuous cuprizone, the remyelination remains limited and does not progress during a recovery interval that was examined out to 6 weeks. This limited remyelination corresponds with depletion of the OP pool ([16] current study). However, the number of oligodendrocytes increases somewhat during the recovery period without a corresponding increase in remyelination of the corpus callosum. Taken together, these findings indicate that the depleted OP pool has a limited capacity to generate oligodendrocytes, and available OP cells may fail to fully differentiate into remyelinating oligodendrocytes in the environment of a chronic lesion. In lesions of some MS cases, immature oligodendrocyte progenitors and premyelinating oligodendrocytes may be present in relatively normal densities without efficiently remyelinating (9, 28). Therefore, further studies will be important for better understanding regulation of the OP pool size and the transition of OP cells into premyelinating and then myelinating oligodendrocytes.

Robust OP proliferation in response to acute demyelination appears to be required for spontaneous remyelination (29). During acute demyelination, the OP pool is dramatically amplified so that efficient differentiation into mature oligodendrocytes may not be required for extensive remyelination. PDGF-AA ligand, acting through *PDGFαR* activation, is an important mitogen for this OP amplification in response to acute cuprizone demyelination (11, 30). In *PDGFαR* heterozygous mice, amplification of the OP pool in response to acute cuprizone demyelination is compromised and the corresponding generation of oligodendrocytes is

reduced (11). Crossing these *PDGFαR* heterozygous mice to *FGF2*$^{-/-}$ mice actually increased oligodendroglial repopulation of lesions after acute cuprizone demyelination (11). Therefore, in both acute and chronic lesion environments, FGF2 removal may promote the generation of oligodendrocytes from OP cells during remyelination.

Endogenous FGF2 has been predicted to contribute to proliferation of neonatal and adult OPs, especially when present in combination with PDGF-AA, based on in vitro studies (31–33). In our current analysis, the densities of OP cells and Ki-67-immunolabeled cells were similar between *FGF2* wild-type and null genotypes. These results are consistent with our previous BrdU incorporation studies indicating that endogenous FGF2 is not a predominant mitogen for OPs in the acute cuprizone model (11). However, subtle changes in the proliferation rate among an asymmetrically dividing OP pool could be relatively difficult to detect in a small population of cells over a prolonged disease and recovery course. FGF2 is also predicted to stimulate neural stem cells in the subventricular zone (SVZ) to contribute to repopulation of corpus callosum lesions (34). During the prolonged demyelination period of the current study, the contribution of cells derived from the SVZ should have been evident in the dynamics of the OP pool in the corpus callosum. The lack of a detrimental effect of FGF2 absence on the OP pool may indicate that FGF2 effects on the SVZ cells may not be a significant contribution to the remyelination of the overlying corpus callosum. However, more direct analysis of the response of cells in the SVZ is required to make this determination. In addition, endogenous elevation of FGF2 in lesions may elicit specific effects that are not replicated with in vivo methods of elevating exogenous FGF2 levels (34–37).

FGF2 is among the most effective neuroprotective growth factors in diverse models of CNS injury, including stroke, trauma, excitotoxicity, and axotomy (38, 39). In contrast to this expected protective effect of FGF2 on neurons, removal of endogenous FGF2 actually improved regenerative parameters in lesions that involved remyelination. Improved regeneration of oligodendrocytes was observed in *FGF2*$^{-/-}$ mice after acute cuprizone demyelination of the corpus callosum and after murine hepatitis virus strain A59 demyelination of spinal cord ([11, 12] current study). In an example from the peripheral nervous system, *FGF2* knockout mice were used to prevent the normal upregulation of FGF2 and FGF receptor (FGFR) activation associated with Schwann cells and macrophages at a site of sciatic nerve crush injury (40). Compared with wild-type mice, the *FGF2* knockout mice exhibited improved myelination and increased axon diameter during regeneration from sciatic nerve crush (40). These results indicate that a detrimental effect of endogenous FGF2 on remyelination may outweigh FGF2 protection from acute axon damage in these lesion models. Indeed, the improved remyelination in nerves of the *FGF2* knockout mice may provide significant protection of axons from damage subsequent to the initial crush injury. Correlative support for a similar role of FGF2 in a chronic autoimmune model of MS can be found in a study of neural stem cell transplantation improved into mice with experimental allergic encephalomyelitis (EAE) (41). The transplanted mice exhibited improved remyelination, with a major contribution from endogenous cells, and had less axonal loss in lesion areas. Neural stem cell transplantation was also associated with a significant decrease in FGF2 expression and reduced astroglial scar formation in the EAE lesions. FGF2 levels may modulate scar formation in demyelinated lesions because expression of FGF2 and FGFR1 corresponds with scarring, but not nonscarring, astroglial responses after other forms of CNS injury (42).

It is not yet clear which FGFR type, or types, mediates the effect of endogenous FGF2 in the context of demyelination and remyelination. Differential effects of FGF2 at different stages of the oligodendrocyte lineage may occur through differential expression and activation of FGFR isoforms (43). Oligodendrocyte lineage cell expression of high-affinity FGFRs and coreceptors varies with developmental stage and FGF2 exposure (44). Furthermore, expression of multiple FGFR types is significantly increased in response to demyelination (19). FGF2 may also have differential effects based on changing interactions with other signaling pathways that regulate oligodendrocyte lineage differentiation and myelination such as Notch1 (45, 46) and neuregulin (47, 48). Interpreting a direct effect of FGF2 is complicated because neurons and glial cells express multiple FGFR types within and near demyelinated lesions (19). Therefore, future studies will be required to identify the specific signaling components mediating endogenous FGF2 signaling in the in vivo context of demyelination and remyelination.

In MS lesions, the pathology is heterogeneous and the effect on the oligodendrocyte lineage population varies dramatically (49). Oligodendrocyte density is severely compromised in demyelinated lesions in some patients with MS. Further studies are imperative to optimize regenerative responses from immature oligodendrocyte lineage cell populations that have been observed in some MS lesions (9, 28). Targeting inhibitory signals that are upregulated in lesions should be a viable strategy for therapeutics to promote differentiation as needed near lesions. FGF2 expression has been reported in reactive astrocytes of acute and chronic MS plaques (50). In addition, in cultures from adult human brain white matter, FGF2 inhibited the differentiation of preoligodendrocytes into oligodendrocytes (51). Strategies to promote remyelination by attenuating FGF2 inhibition of OP differentiation may take advantage of reagents to modulate FGF2 signaling, which are currently being developed for angiogenesis and cancer treatments. In our in vivo analysis, absence of FGF2 was not detrimental in the normal adult or throughout the disease process. Therefore, inhibition of FGF2 signaling may be acceptable across demyelinating disease stages, which would improve treatment feasibility in diseases such as MS that have an unstable disease course. Treatments to promote remyelination should be a valuable complement to strategies that abrogate ongoing causes of demyelination such as immunomodulatory therapies.

ACKNOWLEDGMENTS

The authors thank Dr. Thomas Doetschman for providing breeding pairs of the FGF2 targeted deletion

mice, Drs. William Stallcup and Minetta Gardinier for antibodies, and Drs. Lynn Hudson and William Richardson for plasmids. The authors also thank Drs. Josh Murtie and Nicole Dobson for critical reading of the manuscript.

REFERENCES

1. Prineas JW, Barnard RO, Kwon EE, et al. Multiple sclerosis: Remyelination of nascent lesions. Ann Neurol 1993;33:137–51
2. Raine CS, Wu E. Multiple sclerosis: Remyelination in acute lesions. J Neuropathol Exp Neurol 1993;52:199–204
3. Bruck W, Kuhlmann T, Stadelmann C. Remyelination in multiple sclerosis. J Neurol Sci 2003;206:181–85
4. Chari DM, Blakemore WF. New insights into remyelination failure in multiple sclerosis: Implications for glial cell transplantation. Mult Scler 2002;8:271–77
5. Armstrong RC, Redwine JM, Messersmith DJ. Coronavirus induced demyelination and remyelination: Growth factor expression and function. In: Lavi E, Constantinescu CS, eds. *Experimental Models of Multiple Sclerosis*. New York, NY: Springer 2005:793–803
6. Reynolds R, Cenci di Bello I, Dawson M, et al. The response of adult oligodendrocyte progenitors to demyelination in EAE. Prog Brain Res 2001;132:165–74
7. Watanabe M, Toyama Y, Nishiyama A. Differentiation of proliferated NG2-positive glial progenitor cells in a remyelinating lesion. J Neurosci Res 2002;69:826–36
8. Solanky M, Maeda Y, Ming X, et al. Proliferating oligodendrocytes are present in both active and chronic inactive multiple sclerosis plaques. J Neurosci Res 2001;65:308–17
9. Chang A, Tourtellotte WW, Rudick R, et al. Premyelinating oligodendrocytes in chronic lesions of multiple sclerosis. N Engl J Med 2002; 346:165–73
10. Murtie JC, Zhou YX, Le TQ, et al. In vivo analysis of oligodendrocyte lineage development in postnatal FGF2 null mice. Glia 2005; 49:542–54
11. Murtie JC, Zhou YX, Le TQ, et al. PDGF and FGF2 pathways regulate distinct oligodendrocyte lineage responses in experimental demyelination with spontaneous remyelination. Neurobiol Dis 2005;19: 171–82
12. Armstrong RC, Le TQ, Frost EE, et al. Absence of fibroblast growth factor 2 promotes oligodendroglial repopulation of demyelinated white matter. J Neurosci 2002;22:8574–85
13. Matsushima GK, Morell P. The neurotoxicant, cuprizone, as a model to study demyelination and remyelination in the central nervous system. Brain Pathol 2001;11:107–16
14. Ludwin SK. Chronic demyelination inhibits remyelination in the central nervous system. An analysis of contributing factors. Lab Invest 1980; 43:382–87
15. Tansey FA, Zhang H, Cammer W. Expression of carbonic anhydrase II mRNA and protein in oligodendrocytes during toxic demyelination in the young adult mouse. Neurochem Res 1996;21:411–16
16. Mason JL, Toews A, Hostettler JD, et al. Oligodendrocytes and progenitors become progressively depleted within chronically demyelinated lesions. Am J Pathol 2004;164:1673–82
17. Zhou M, Sutliff RL, Paul RJ, et al. Fibroblast growth factor 2 control of vascular tone. Nat Med 1998;4:201–7
18. Redwine JM, Armstrong RC. In vivo proliferation of oligodendrocyte progenitors expressing PDGFalphaR during early remyelination. J Neurobiol 1998;37:413–28
19. Messersmith DJ, Murtie JC, Le TQ, et al. Fibroblast growth factor 2 (FGF2) and FGF receptor expression in an experimental demyelinating disease with extensive remyelination. J Neurosci Res 2000;62: 241–56
20. Hudson LD, Berndt JA, Puckett C, et al. Aberrant splicing of proteolipid protein mRNA in the dysmyelinating jimpy mutant mouse. Proc Natl Acad Sci U S A 1987;84:1454–58
21. Fruttiger M, Karlsson L, Hall AC, et al. Defective oligodendrocyte development and severe hypomyelination in PDGF-A knockout mice. Development 1999;126:457–67
22. Linnington C, Webb M, Woodhams PL. A novel myelin-associated glycoprotein defined by a mouse monoclonal antibody. J Neuroimmunol 1984;6:387–96
23. Gerdes J, Lemke H, Baisch H, et al. Cell cycle analysis of a cell proliferation-associated human nuclear antigen defined by the monoclonal antibody Ki-67. J Immunol 1984;133:1710–15
24. Mason JL, Langaman C, Morell P, et al. Episodic demyelination and subsequent remyelination within the murine central nervous system: Changes in axonal calibre. Neuropathol Appl Neurobiol 2001;27: 50–58
25. Mallon BS, Shick HE, Kidd GJ, et al. Proteolipid promoter activity distinguishes two populations of NG2-positive cells throughout neonatal cortical development. J Neurosci 2002;22:876–85
26. Song SK, Yoshino J, Le TQ, et al. Demyelination increases radial diffusivity in mouse brain white matter. Neuroimage 2005;26: 132–40
27. Steward O, Schauwecker PE, Guth L, et al. Genetic approaches to neurotrauma research: Opportunities and potential pitfalls of murine models. Exp Neurol 1999;157:19–42
28. Maeda Y, Solanky M, Menonna J, et al. Platelet-derived growth factor-alpha receptor-positive oligodendroglia are frequent in multiple sclerosis lesions. Ann Neurol 2001;49:776–85
29. Keirstead HS, Blakemore WF. The role of oligodendrocytes and oligodendrocyte progenitors in CNS remyelination. Adv Exp Med Biol 1999;468:183–97
30. Woodruff RH, Fruttiger M, Richardson WD, et al. Platelet-derived growth factor regulates oligodendrocyte progenitor numbers in adult CNS and their response following CNS demyelination. Mol Cell Neurosci 2004;25:252–62
31. McKinnon RD, Matsui T, Dubois-Dalcq M, et al. FGF modulates the PDGF-driven pathway of oligodendrocyte development. Neuron 1990; 5:603–14
32. Wolswijk G, Noble M. Cooperation between PDGF and FGF converts slowly dividing O-2A adult progenitor cells to rapidly dividing cells with characteristics of O-2Aperinatal progenitor cells. J Cell Biol 1992; 118:889–900
33. Frost EE, Nielsen JA, Le TQ, et al. PDGF and FGF2 regulate oligodendrocyte progenitor responses to demyelination. J Neurobiol 2003;54:457–72
34. Decker L, Picard-Riera N, Lachapelle F, et al. Growth factor treatment promotes mobilization of young but not aged adult subventricular zone precursors in response to demyelination. J Neurosci Res 2002;69:763–71
35. Ruffini F, Furlan R, Poliani PL, et al. Fibroblast growth factor-II gene therapy reverts the clinical course and the pathologic signs of chronic experimental autoimmune encephalomyelitis in C57BL/6 mice. Gene Ther 2001;8:1207–13
36. Lachapelle F, Avellana-Adalid V, Nait-Oumesmar B, et al. Fibroblast growth factor-2 (FGF-2) and platelet-derived growth factor AB (PDGF AB) promote adult SVZ-derived oligodendrogenesis in vivo. Mol Cell Neurosci 2002;20:390–403
37. Butt AM, Dinsdale J. Fibroblast growth factor 2 induces loss of adult oligodendrocytes and myelin in vivo. Exp Neurol 2005;192:125–33
38. Teng YD, Mocchetti I, Taveira-DaSilva AM, et al. Basic fibroblast growth factor increases long-term survival of spinal motor neurons and improves respiratory function after experimental spinal cord injury. J Neurosci 1999;19:7037–47
39. Alzheimer C, Werner S. Fibroblast growth factors and neuroprotection. Adv Exp Med Biol 2002;513:335–51
40. Jungnickel J, Claus P, Gransalke K, et al. Targeted disruption of the FGF-2 gene affects the response to peripheral nerve injury. Mol Cell Neurosci 2004;25:444–52
41. Pluchino S, Quattrini A, Brambilla E, et al. Injection of adult neurospheres induces recovery in a chronic model of multiple sclerosis. Nature 2003;422:688–94
42. Smith C, Berry M, Clarke WE, et al. Differential expression of fibroblast growth factor-2 and fibroblast growth factor receptor 1 in a scarring and nonscarring model of CNS injury in the rat. Eur J Neurosci 2001;13:443–56
43. Fortin D, Rom E, Sun H, et al. Distinct fibroblast growth factor (FGF)/FGF receptor signaling pairs initiate diverse cellular responses in the oligodendrocyte lineage. J Neurosci 2005;25:7470–79

44. Bansal R, Kumar M, Murray K, et al. Developmental and FGF-2-mediated regulation of syndecans (1–4) and glypican in oligodendrocytes. Mol Cell Neurosci 1996;7:276–88
45. Wang S, Sdrulla AD, diSibio G, et al. Notch receptor activation inhibits oligodendrocyte differentiation. Neuron 1998;21:63–75
46. John GR, Shankar SL, Shafit-Zagardo B, et al. Multiple sclerosis: Re-expression of a developmental pathway that restricts oligodendrocyte maturation. Nat Med 2002;8:1115–21
47. Viehover A, Miller RH, Park SK, et al. Neuregulin: An oligodendrocyte growth factor absent in active multiple sclerosis lesions. Dev Neurosci 2001;23:377–86
48. Sussman CR, Vartanian T, Miller RH. The ErbB4 neuregulin receptor mediates suppression of oligodendrocyte maturation. J Neurosci 2005;25:5757–62
49. Lucchinetti C, Bruck W, Parisi J, et al. A quantitative analysis of oligodendrocytes in multiple sclerosis lesions. A study of 113 cases. Brain 1999;122:2279–95
50. Holley JE, Gveric D, Newcombe J. Astrocyte characterization in the multiple sclerosis glial scar. Neuropathol Appl Neurobiol 2003;29:434–44
51. Armstrong RC, Dorn HH, Kufta CV. Pre-oligodendrocytes from adult human CNS. J Neurosci 1992;12:1538–47